RSC Advances

PAPER

View Article Online
View Journal | View Issue

Cite this: *RSC Adv.*, 2025, **15**, 3988

Influence of metal doping on the coke formation of a novel hierarchical HZSM-5 zeolite catalyst in the conversion of 1-propanol to fuel blendstock†

Ifeanyi Michael Smarte Anekwe * and Yusuf Makarfi Isa

In this work, the effect of Ni doping on coke formation and the activity of a novel hierarchical HZSM-5 zeolite catalyst in the conversion of 1-propanol to fuel blends was investigated. The catalysts, which were hydrothermally synthesised and modified with 0.5 wt% Ni, were characterised using different techniques (XRD, FTIR, SEM, PSD, N_2 adsorption, NH_3-TPD, TGA-DTA) and tested at 350–400 °C and, WHSV of 7 and 12 h^{-1} for the conversion of 1-propanol into fuel blendstocks. The catalyst characterisation results confirmed the successful synthesis of hierarchical HZSM-5 and the incorporation of nickel. The catalytic results showed that both catalysts exhibited >98% 1-propanol conversion with considerable selectivity (>80%) for jet fuel and (>50%) gasoline blendstock. While Ni/HZSM-5 favoured jet fuel, the undoped catalyst improved gasoline production. The stability and deactivation study showed that HZSM-5 exhibited greater long-term stability and maintained a conversion rate of >95%, making it well-suited for the extended conversion of 1-propanol. The moderate production of jet fuel and the uniform selectivity of gasoline indicate a balanced distribution of products. In contrast, Ni/HZSM-5 initially provides higher jet fuel production and stable gasoline production, but the conversion rate drops more sharply after 40 h on stream, which is due to rapid deactivation by coke accumulation or deactivation of metal sites. The coking study showed that the Ni-doped catalysts produced more coke, resulting in a weight loss of 6.4 wt% compared to the unmodified catalysts (6.1 wt%), which contributed to their deactivation, as evidenced by a reduction in 1-propanol conversion. Characteristic spectral bands from the analysis of the spent catalysts indicated the composition of the coke present, with key regions at 1300–1700 cm^{-1} and 2800–3100 cm^{-1} showing that the spent catalysts consisted of polycondensed aromatics, conjugated olefins and aliphatics. It can be concluded that the metal modification improves the catalytic performance but increases the coking and deactivation tendencies compared to the unmodified catalyst, which may limit the stability of the catalyst.

Received 28th October 2024
Accepted 20th January 2025

DOI: 10.1039/d4ra07707e

rsc.li/rsc-advances

1. Introduction

According to the U.S. Energy Information Administration (EIA), global energy consumption will increase by 2050 and overtake progress in energy efficiency. In recent decades, efforts have been made worldwide to research sustainable, economically viable and energy-efficient methods of producing fuels and chemicals. In the face of dwindling reserves and increasing environmental concerns,[1] renewable energy sources such as lignocellulosic biomass have proven to be an abundant and sustainable source of organic carbon worldwide. Utilising biomass for the production of biofuels or biochemical products is a promising way to replace fossil products and achieve sustainability. In addition, biomass resources are currently underutilised, and the establishment of biorefineries holds the potential for societal benefits such as strengthening the rural economy and diversifying and securing energy resources.[2,3] Numerous technologies have been developed to convert biomass or its derivatives into fuels and chemicals, with catalysis playing a central role.[2,4–6]

Different catalysts have been employed in the conversion of propanol to HCs, including zeolite catalysts,[7–9] metal-doped catalysts,[8] metal-containing mesoporous silica-based materials[10] among others. Ramasamy and Wang[11] investigated the conversion of alcohols into transportation fuel-range hydrocarbons using HZSM-5 catalyst ($SiO_2/Al_2O_3 = 30$) at 360 °C and 300 psig. The study revealed that the catalyst lifespan was more than twice as long for 1-propanol and 1-butanol compared to methanol and ethanol. After 24 h time on stream (TOS), the liquid products from the transformation of 1-propanol and 1-butanol primarily consisted of higher olefin compounds.[11] Lepore, Li[8] demonstrated that HZSM-5 zeolite catalysts possess

School of Chemical and Metallurgical Engineering, University of the Witwatersrand, Johannesburg 2050, South Africa. E-mail: Ifeanyi.anekwe@wits.ac.za; anekwesmarte@gmail.com

† Electronic supplementary information (ESI) available. See DOI: https://doi.org/10.1039/d4ra07707e

significant versatility in improving the conversion of 1-propanol into hydrocarbons. Their research indicated that raising the reaction temperature beyond 230 °C shifted the product distribution towards C_4^+ liquid HCs, promoting oligomerisation. In contrast, maintaining the temperature at 230 °C or lower favoured dehydration reactions and enhanced propene selectivity.[8] In their study, Mentzel, Shunmugavel[12] investigated the conversion of isopropanol over HZSM-5 zeolite catalysts at temperatures of 400 °C and pressures ranging from 1 to 20 bar. They observed conversion rates between 40% and 80%, with selectivity for C_5^+ liquid HCs ranging from 35% to 60%. Notably, at a pressure of 20 bar, the liquid product, after about one-third of the reaction time, primarily consisted of C_4–C_{12} alkenes. The study highlighted that the catalyst's longevity when converting isopropanol was significantly better than when using other alcohols, while the selectivity of liquid products is closely tied to the weight hourly space velocity (WHSV). It was found that both the lifespan and conversion efficiency of the zeolite catalyst improved markedly when isopropanol was employed as the feedstock, compared to methanol or ethanol.[12] In addition, metal modifications including Ni, Fe, Co and Ga have been shown to promote the conversion of biomass derivatives, including alcohol, into liquid HCs.[9,13–17]

Catalysts and operating conditions that favour the selectivity of long-chain hydrocarbons lead to faster deactivation compared to conventional systems.[18] Guisnet and Magnoux[19] proved that both the pore framework of the zeolite and the operating conditions influence coking and subsequent deactivation in equal measure. At lower temperatures, coke deposition is mainly due to condensation and rearrangement processes. At temperatures above 350 °C, however, coke formation is also influenced by hydrogen transfer. The deactivation rates in different zeolite structures are significantly affected by the crystal size, the strength of the acid sites and the concentration.[20] Two systematic studies have correlated the deactivation rates with the synthesis of polycyclic aromatic compounds.[21,22] Based on these correlations, it was assumed that coke generation takes place predominantly on the outer surface of the zeolite crystals.[18,23–25] However, it has also been theorised that coke formation on the outside of the catalyst only occurs when the catalyst becomes inactive due to pore-clogging coke formation on the inside.[26] However, Bjørgen, Svelle[27] found no link between the content of organic molecules trapped in the pores and the deactivation of the zeolite at 350 °C. They inferred that the decrease in activity with time in the stream was due to coke deposition on the outer surface, which is consistent with Schulz[28] results. The characterisation of a deactivated sample for a certain duration does not provide detailed insights into the chemistry of the deactivation, as the sample contains various coke deposits from several reactions. Bleken, Barbera[29] studied this problem by dividing the catalyst bed into sections and analysing each separately. They reported an increase in the weight or density of the coke species as the catalyst bed sank downwards, indicating different chemical reactions responsible for carbonaceous deposits depending on the nature of the catalyst bed. Measures such as feedstock pretreatment, catalyst enhancement and catalyst rejuvenation have been developed to address deactivation issues. However, further research is required to fully understand catalyst deactivation and to develop strategies to minimise its effects.

Therefore, this work uniquely evaluates the effect of metal incorporation on stability and coke formation by employing a newly developed hierarchical HZSM-5 zeolite catalyst specifically for the conversion of 1-propanol to fuel-range hydrocarbons, unlike previous studies that focused on microporous or commercial ZSM-5 or other heterogeneous catalysts for this conversion. The hierarchical structure in the newly developed HZSM-5 catalyst was designed to enhance diffusion and prevent coke buildup within micropores, an issue that limited the lifespan of traditional zeolites in earlier studies. Additionally, nickel doping was employed to optimise hydrogen transfer reactions, allowing efficient liquid HC production. A range of physicochemical techniques were used to characterise both the fresh and spent catalyst, providing crucial insights into catalyst stability and coke deposition for an informed discussion.

2. Materials and methods

The following chemicals were employed for this study: $(Na_2O)SiO_2.H_2O$, $Al_2(SO_4)_3 \cdot 18H_2O$, $C_{12}H_{28}BrN$, NaOH: 97%, H_2SO_4: 98% conc. and NH_4NO_3. $Ni(NO_3)_2 \cdot 6H_2O$ was used as Ni precursor while 1-propanol was used as the feedstock. These chemicals were procured from Sigma-Aldrich. A stainless steel hydrothermal reactor with a Teflon cup of 200 mL was used for catalyst preparation.

2.1. Fresh catalyst preparation and characterisation

The newly developed hierarchical ZSM-5 catalyst support was synthesised using the hydrothermal catalyst synthesis method described in our previous study.[15] The batch formula comprised $10Na_2O$, $40SiO_2$, $1.0Al_2O_3$, 10.5TPABr and $3740.6H_2O$. Three solutions were prepared: the first contained the required amount of $(Na_2O)SiO_2 \cdot H_2O$ and NaOH, the second contained tetrapropylammonium bromide, and the third contained 3.80 g aluminium sulphate. After mixing and stirring, sulphuric acid (98%) was added to adjust the pH to 10.73. The gel was then hydrothermally crystallised at 180 °C for 24 hours, filtered, washed, dried at 110 °C and calcined at 550 °C for 3 h. After ion exchange with NH_4NO_3, drying and calcination at 550 °C for 6 hours, the resulting NH_4^+/ZSM-5 was modified with 0.5 wt% nickel nitrate by dry impregnation. The modified catalyst, designated as Ni/HZSM-5, was dried and calcined at 550 °C for 6 h.

The crystallinity of the fresh catalysts was analysed using a Bunker D2 phase diffractometer. Cu Kα radiation at 40 kV and 30 mA was used, with a sampling rate of 2° per minute. The identification of functional groups of fresh catalysts was conducted with a PerkinElmer Fourier Transform-Attenuated Total Reflectance-Infrared Spectrometer Spectrum-2 operating in the range of 4000–400 cm^{-1}. The textural properties of the catalysts were determined using an N_2 adsorption–desorption analyser after 6 hours of degassing at 400 °C. Morphological analysis was

performed by scanning electron microscopy using a ZEISS Sigma 300 VP, while the particle size distribution (PSD) was recorded using a Malvern instrument. The elemental composition of the catalysts was carried out using energy-dispersive X-ray spectroscopy (EDS) and X-ray fluorescence techniques. NH_3-TPD analysis was performed on an AutoChem II 2920 chemisorption analyser to determine the catalyst's acidity. The sample was heated at a rate of 10 °C min^{-1} up to 700 °C to remove adsorbed water while a TCD detector monitored the NH_3 desorption signal. The characterisation results of fresh catalyst can be found in the ESI.†

2.2. Catalyst evaluation for 1-propanol conversion and product analysis

The catalyst was tested in the transformation of 1-propanol to hydrocarbons at 350 and 400 °C, and a Weight Hourly Space Velocity (WHSV) of 7 and 12 h^{-1} using 0.4–0.5 g catalyst. Catalyst stability study was conducted at 7 h^{-1} and 350 °C for 40 h time on stream (TOS). After the initial activation of the catalyst at 400 °C for 40 min, 1-propanol was introduced at 0.075–0.125 mL min^{-1} into the stainless steel fixed-bed reactor, which had an inner diameter of 1.02 cm and a length of 64.52 cm, using an HPLC pump. Glass beads and wool provided structural support for the catalyst bed.

A YL6500 gas chromatograph (GC) system, equipped with a Flame Ionization Detector (FID) and a capillary column, was used to analyse hydrocarbons. The column program was as follows: the sample was initially injected at 40 °C, then the column was heated at 3 °C per minute to reach 50 °C and held for 3 minutes. Next, the temperature was increased at a rate of 2 °C per minute to 60 °C and maintained for 1 minute. The column was then heated at 5 °C per minute until reaching 200 °C, where it was held for 1 minute. Finally, the temperature was raised to 315 °C at 15 °C per minute and held for 5 minutes. In the conversion of 1-propanol to fuel blendstock, the product mixture can be categorized into distinct "product lumps," comprising light hydrocarbons (C_1–C_4), fuel-range hydrocarbons (C_5^+), including gasoline-range hydrocarbons (C_5–C_8) and jet-fuel-range hydrocarbons (C_9–C_{16}), and, in some cases, aromatics or other heavy hydrocarbons (C_{16}^+). The product selectivity (S) and 1-propanol conversion (X) were determined based on the study by Sun, Ma[30] as shown in eqn (1) and (2).

$$X = \frac{\text{Amount of reacted 1-propanol}}{\text{Initial amount of 1-propanol}} \times 100\% \quad (1)$$

$$S = \frac{\text{Amount of produced fuel-range HC}}{\text{Amount of reacted 1-propanol}} \times 100\% \quad (2)$$

2.3. Spent catalyst characterisation (coke analysis)

XRD and SEM analyses were conducted to examine changes in crystallinity and morphology of the spent catalysts, following the procedure described in Section 2.1. Functional groups in the coke deposited on spent catalysts were identified using a PerkinElmer Spectrum-2 Fourier Transform-Attenuated Total Reflectance Infrared (FT-ATR-IR) spectrometer, operating within the range of 4000 to 400 cm^{-1}. Thermogravimetric/differential thermal analysis (TGA/DTA) was performed to determine weight loss (due to the amount of coke deposition on spent catalysts) using a TA Instrument Q50 USA thermal analyser covering a temperature range of 30 to 800 °C with a heating rate of 15 °C per minute. The sample was thermally treated in an N_2 atmosphere (flow rate: 50 mL min^{-1}) from 30 °C to 200 °C, then switched to air and further heated to 800 °C.

3. Results and discussion

3.1. Catalyst evaluation in the conversion of 1-propanol to fuel blendstocks

3.1.1. Effect of operating conditions in 1-propanol conversion and product distribution. The conversion of 1-propanol to fuel blendstocks was investigated at weight hourly space velocities (WHSV) of 7 and 12 h^{-1}, and temperatures of 350 and 400 °C. Fig. 1a–c present the 1-propanol conversion and the selectivity of individual catalysts for gaseous and liquid HC products. Results showed that all catalysts achieved over 98% 1-propanol conversion, producing broad product distributions with a notable preference for gaseous products at a WHSV of 7 h^{-1} and more liquid products at 12 h^{-1} (Fig. 1c). At 350 °C and a WHSV of 7 h^{-1}, the HZSM-5 catalyst exhibited the highest selectivity for gasoline (42.39%), while Ni/HZSM-5 showed increased selectivity towards BTX (12.40%). However, the production of jet fuel remained low under these conditions for both catalysts, with yields below 30%. Raising the temperature while maintaining the same WHSV resulted in a slight increase in the production of BTX, gasoline, and jet fuel for the Ni/HZSM-5 catalyst, accompanied by a decrease in gaseous HC yields. The undoped catalyst, however, did not exhibit significant changes with this change in operating condition. In contrast, increasing the WHSV to 12 h^{-1} led to a significant reduction in gaseous HC selectivity and a corresponding increase in gasoline and jet fuel production at 350 °C, achieving 68.79% and >90% selectivity for HZSM-5 and Ni/HZSM-5, respectively. In addition, when the temperature was raised to 400 °C under the same WHSV, there were slight shifts in product distribution, with both gasoline and jet fuel production improving. Specifically, HZSM-5 and Ni/HZSM-5 recorded selectivity of 84.97% and 53.70%, respectively. These findings indicate that Ni doping in the catalyst reduced C_1–C_4 HC production while increasing selectivity for C_5^+ liquid hydrocarbons. This behaviour can be attributed to the enhanced oligomerisation reactions facilitated by Ni incorporation during the initial stages of the dehydration process.[31]

The conversion of alcohols to hydrocarbons has been extensively studied using various catalysts, with zeolites and modified zeolites being the most employed.[32–36] Depending on the catalyst, different reaction mechanisms have been proposed. For ZSM-5 zeolite catalysts, the mechanism is thought to involve intermediate species, with hydrocarbons forming through secondary reactions.[36,37] In this study, we hypothesise that 1-propanol first undergoes dehydration to form olefins, which are subsequently converted into

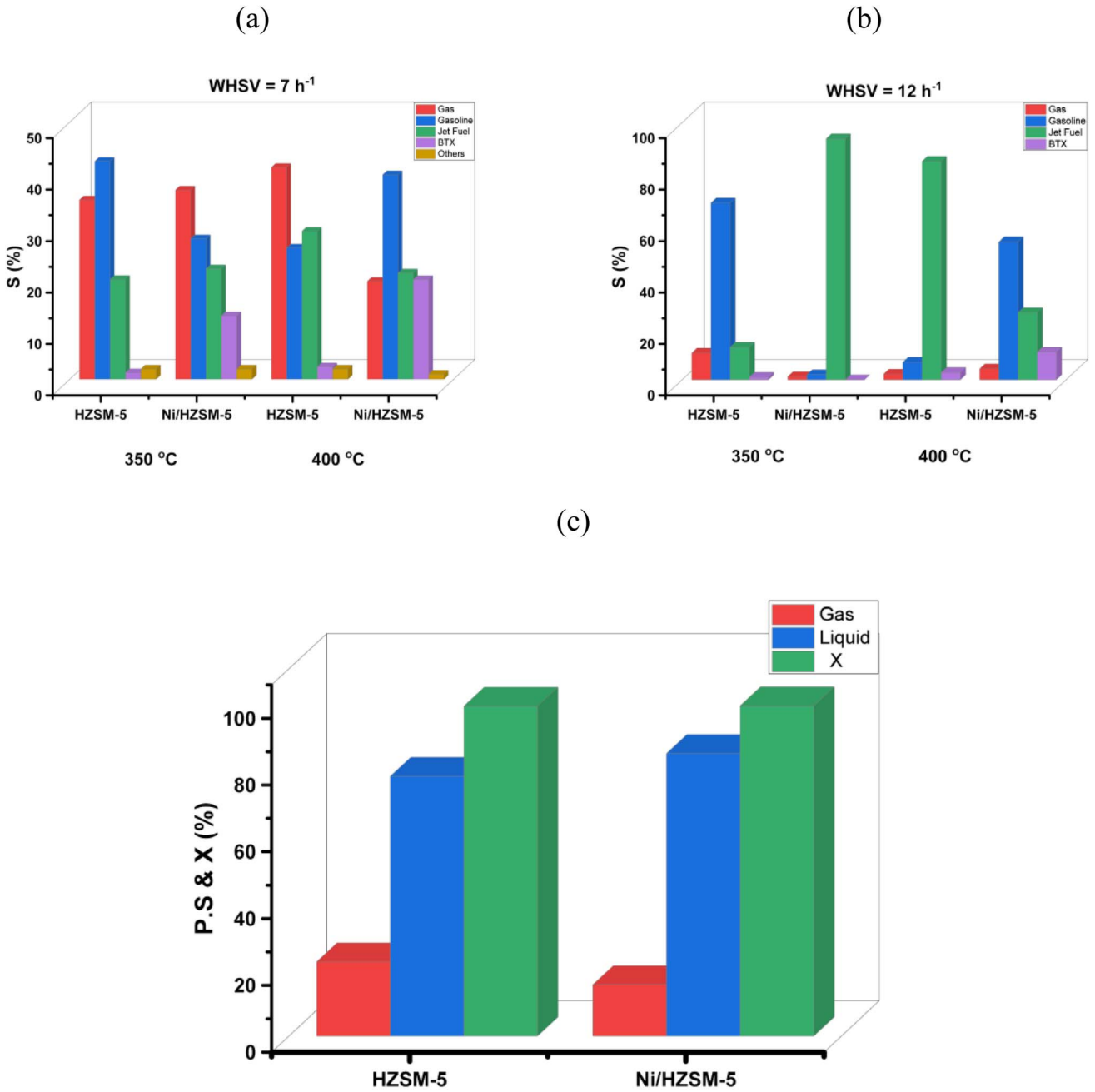

Fig. 1 Product selectivity (S) over HZM-5 and Ni/HZSM-5 at (a) 7 h^{-1} and (b) 12 h^{-1} WHSV (c) average phase selectivity (P.S) and conversion (X) from the 1-propanol conversion to fuel blendstock. Reaction conditions: 350 and 400 °C; WHSV = 7 and 12 h^{-1}.

hydrocarbons (such as C_3^+ olefins, BTX, and C_5^+) through acid-catalysed oligomerisation–cracking and oligomerisation–aromatisation pathways (Fig. 2).[36,37]

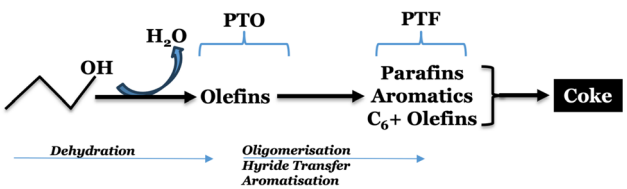

Fig. 2 Reaction pathway for the conversion of 1-propanol to olefin (PTO) and to fuel blendstock (PTF).

3.1.2. Catalyst stability study. The stability study for both hierarchical catalysts showed that the initial conversion of 1-propanol was close to 100%, with a gradual decline observed over time. For HZSM-5, the conversion slightly decreases, reaching 97.5% after 40 h. Ni/HZSM-5, however, shows a more significant drop in conversion, falling to 77.5% by the 40 h mark (Fig. 3a). This suggests that HZSM-5 maintains higher stability in terms of conversion over extended reaction times compared to Ni/HZSM-5. The presence of nickel in Ni/HZSM-5 likely contributes to an initial high catalytic activity but may also lead to faster deactivation over time, potentially due to coke formation or other structural changes affecting active sites.

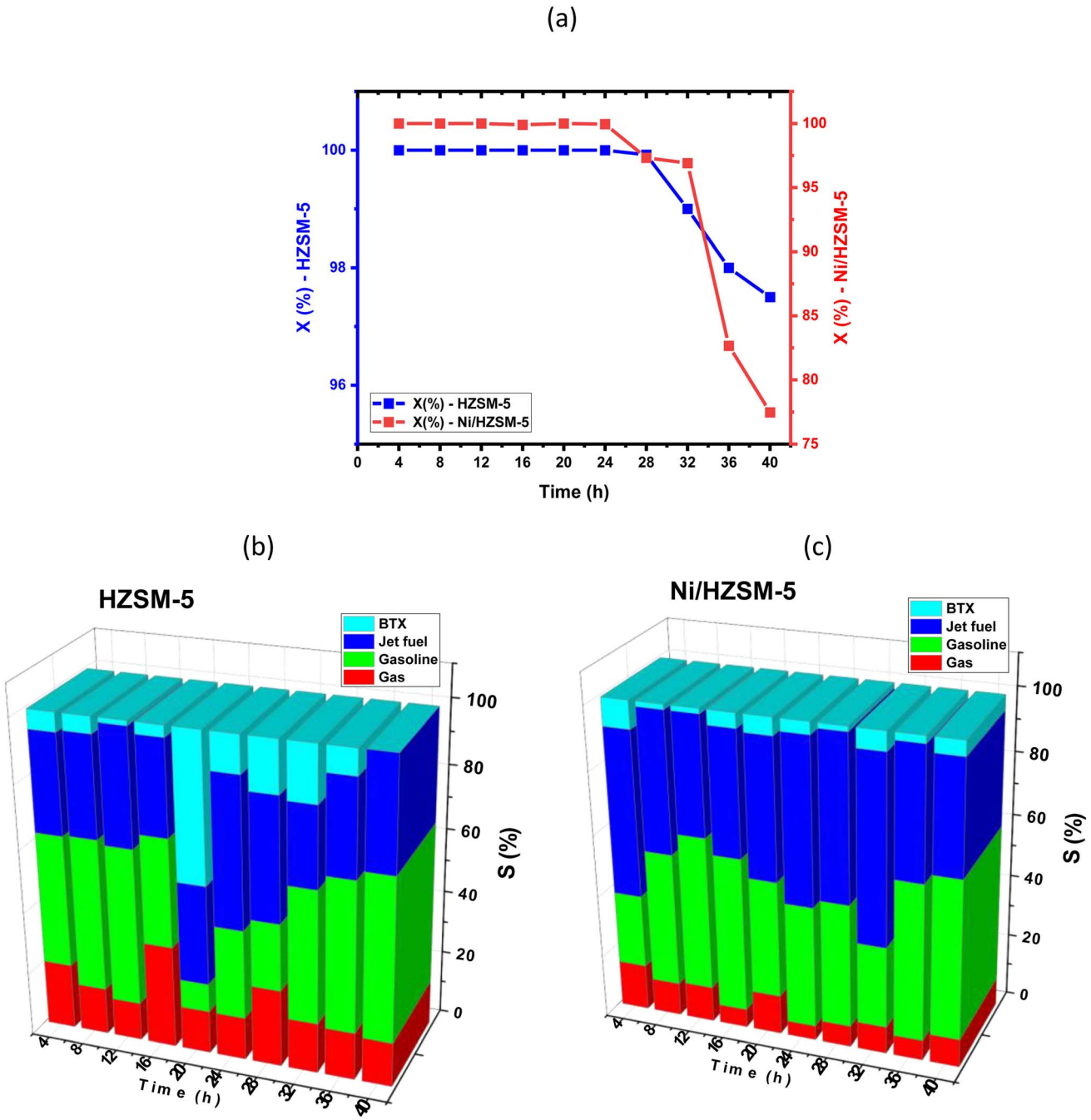

Fig. 3 Catalyst stability study at 7 h^{-1} and 350 °C for 40 h TOS showing (a) 1-propanol conversion (*X*), and product distribution for (b) HZSM-5 (c) Ni/HZSM-5 catalysts.

Both catalysts show distinctive trends in product distribution over time. Both catalysts, HZSM-5 and Ni/HZSM-5, exhibit distinct trends in product distribution over time. For HZSM-5, gas production fluctuates notably, starting at 20.67% and peaking at 32.24% at 16 h, then stabilizing around 13–15% by 40 h (Fig. 3b). In contrast, Ni/HZSM-5 shows lower initial gas production (14.68%) and maintains a relatively low, stable gas yield, suggesting a more efficient conversion of 1-propanol into liquid HCs, particularly jet fuel (Fig. 3c). Gasoline selectivity in HZSM-5 generally increases over time, peaking at 51.12% by 40 h, indicating a gradual shift toward gasoline production. Ni/HZSM-5 follows a similar trend, reaching a peak of 50.53% at 40 h, although it maintains a more stable gasoline selectivity compared to the fluctuations observed with HZSM-5. For jet fuel production, HZSM-5 starts with selectivity around 31–32% and gradually rises to 47.02% at 24 h before levelling off at 35% by 40 h. Ni/HZSM-5, however, consistently produces higher jet fuel, peaking at 59.47% around 32 h, indicating its suitability for prolonged jet fuel production. Regarding aromatic compounds (BTX), HZSM-5 begins with a BTX content of 5.9 7% but reaches a maximum of 46.57% at 20 h before eventually dropping by 40 h. In contrast, Ni/HZSM-5 sustains a low but steady BTX output (1.7–8.85%)

throughout the reaction. This consistent BTX production suggests that Ni/HZSM-5 may better maintain aromatic stability, though it could also contribute to coke formation over time, affecting its overall stability. In addition, the resultant liquid product, which has a very low aromatic content, presents a valuable raw material for the chemical industry and could be readily applied or blended to serve as high-quality clean fuels, similar to the results obtained by other studies.[12,38–40]

HZSM-5 demonstrates a higher long-term stability in conversion rates, making it more suitable for prolonged use in 1-propanol conversion. Its lower jet fuel and consistent gasoline yields suggest a balanced distribution across product types. Ni/HZSM-5, on the other hand, provides a higher initial yield of jet fuel and shows enhanced stability in gasoline production but experiences a sharper decline in conversion, likely due to faster deactivation from coke buildup or metal site deactivation.

3.2. Characterisation of spent catalysts and coke deposition study

3.2.1. Phase identification, morphology, and textural properties of spent catalysts. The XRD spectra of the spent catalysts showed that the intensity of the diffraction peaks did not change significantly after 1-propanol conversion, even when coke deposits were present (Fig. 4). This indicates that the MFI zeolite framework was still intact after catalytic activity, as no breakdown of the framework was observed after the reaction. These results showed that the presence of active Ni metal contributes to the stabilisation of the zeolite structure and could, therefore, reduce the likelihood of framework collapse. In addition, the SEM images (Fig. 5) of the spent catalysts show that the coke deposits on the catalyst surface have not changed the morphology of the catalyst. However, the presence of reactive metals can influence the formation and distribution of the coke deposits on the catalyst surface and, thus, possibly change the surface properties of the modified catalyst.

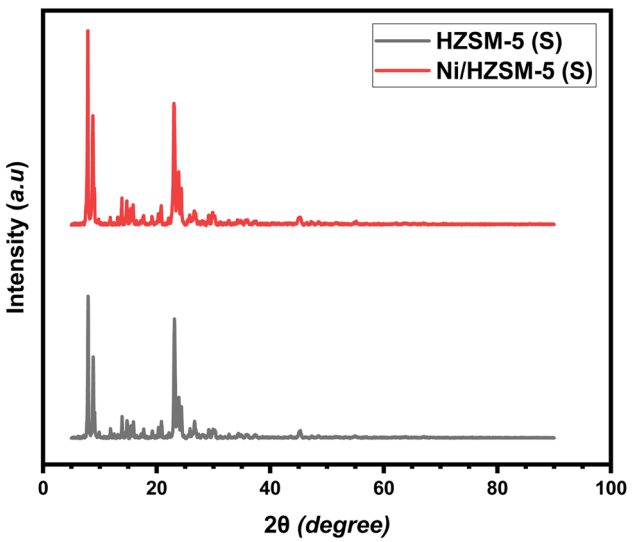

Fig. 4 XRD pattern of spent HZSM-5 and Ni/HZSM-5 catalysts.

Similar to the fresh catalyst (Fig. S4, ESI†), all isotherms for the spent catalyst displayed a combination of type IV isotherms and H4 hysteresis loops,[46,47] occurring at a pressure, $P/P_0 > 0.4$ which indicates the presence of a hierarchically porous structure comprising mesopores and macropores.[41] However, adsorbate uptake at $P/P_0 > 0.4$ decreased drastically for the spent samples to 37.5 and 18.4 $cm^3\ g^{-1}$ for the spent HZSM-5 and Ni/HZSM-5, respectively, compared to the pure samples (Fig. 6). The reduction in surface area corresponded with increased coke deposition, with spent Ni/HZSM-5 decreasing by 85.5% compared to 71.5% for spent HZSM-5, hence, the incorporation of metal species further reduces the total surface area available for adsorption due to increased coke deposition[42,43] (Table 1). This result correlates with the TGA results, which indicate that catalysts with larger coke deposits have a lower surface area. The decrease in mesopores and total pore volume of spent catalysts could be attributed to 1-propanol conversion, coke formation and subsequent pore plugging. Despite the decrease in pore volume, the catalysts still maintain their hierarchical macro–mesoporous nature. Complex reactions during 1-propanol conversion, such as oligomerisation and dehydration, contribute to pore plugging and surface area reduction, as long-chain molecules tend to cover the active sites and hinder access. The formation of aromatic molecules and coke deposits from secondary reactions further reduces the mesopore volume and surface area and limits the availability of reactants at the active sites.[44,45]

The study by Díaz, Epelde[46] has shown that in addition to the reduction in surface area,[47] coke deposition also decreases the HZSM-5 catalyst's total acidity, primarily by blocking the active acidic sites and causing pore obstruction. This buildup of

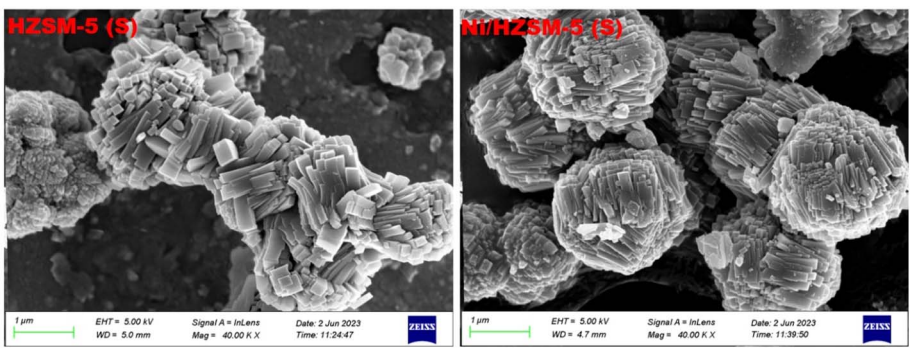

Fig. 5 SEM of spent HZSM-5 and Ni/HZSM-5 catalysts.

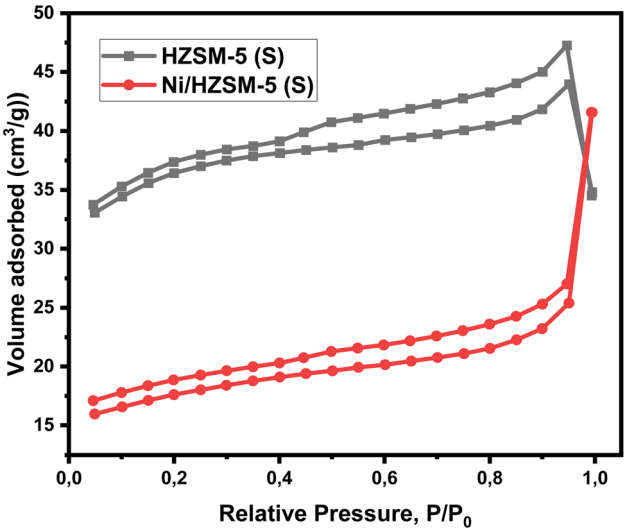

Fig. 6 N_2 adsorption–desorption isotherm for spent catalysts.

carbonaceous deposits, especially near or on the Brønsted acid sites, reduces the number of available acid sites and restricts access to the catalyst's internal surface area.[46] Consequently, the catalytic activity decreases as fewer acid sites are available for reaction, leading to reduced conversion efficiency and selectivity over time. Moreover, coke deposition can alter the strength of the remaining acid sites, often causing a loss in both strong and weak acid sites.[46,48] This deactivation reduces the catalyst's ability to drive desired reactions, especially those requiring high acidity, such as the formation of hydrocarbons in alcohol conversion processes. The extent of deactivation depends on factors like coke composition, reaction conditions, and the catalyst's structure.

3.2.2. Coke amount: TGA-DTA results. Coke formation on spent catalysts was studied by TGA-DTA analysis. The deposition of carbonaceous species on the surface of the catalyst is a common phenomenon in catalytic processes with hydrocarbons. At T = 0–200 °C, the initial weight loss is due to the elimination of absorbed water and volatile compounds. During 1-propanol conversion, both catalysts have a considerable surface area, which enhances the adsorption of H_2O and volatile compounds. The weight loss in this temperature range is considered normal and has nothing to do with the accumulation of coke. Due to its high acidity, the HZSM-5 is known to promote coke deposition during 1-propanol conversion. As a result of the burning of soft and hard coke, the HZSM-5 catalyst showed weight losses of 2.80% and 2.24% at 200 to 400 °C and 400 to 600 °C, respectively (Fig. 7). The elimination of non-volatile molecules from the 1-propanol conversion process was responsible for the observed weight loss of the spent catalysts at 600–800 °C. The acidity of the HZSM-5 contributes to the observed coke deposition, as it facilitates

Table 1 Textural properties of pure and spent catalysts

Catalysts	S_{BET} ($m^2\ g^{-1}$)	$V_{total(BJH)}$ ($cm^3\ g^{-1}$)	$V_{meso(BJH)}$ ($cm^3\ g^{-1}$)	$V_{macro(BJH)}$ ($cm^3\ g^{-1}$)	Avg pore dia. (nm)	Volume@STP ($cm^3\ g^{-1}$)	Metal loading (wt%)
HZSM-5 (S)	113.23	0.669	0.039	0.630	40.03	37.50	0.0
Ni/HZSM-5 (S)	55.43	0.202	0.176	0.026	4.65	18.41	0.5

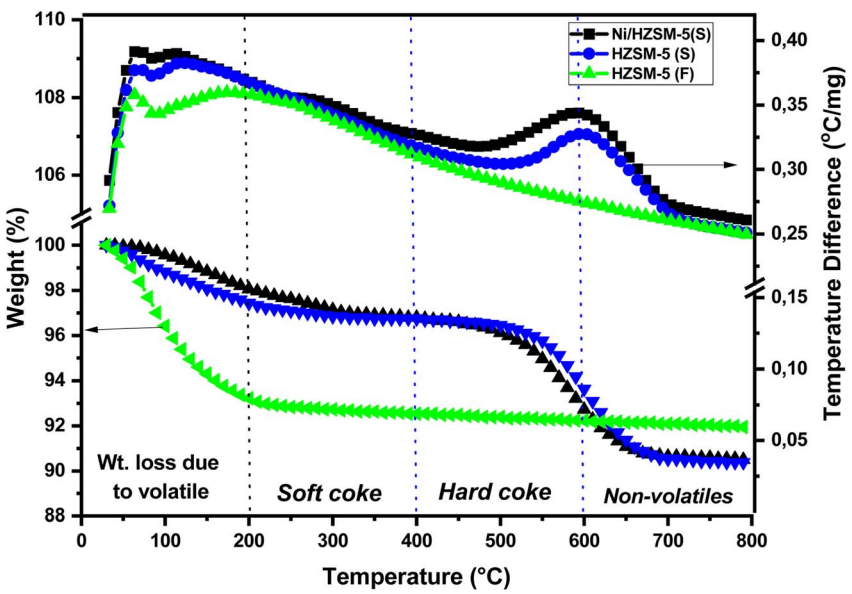

Fig. 7 TGA-DTA of spent HZSM-5 and Ni/HZSM-5 catalysts.

Table 2 Coke deposition (wt%)–summary

Catalysts	Volatiles	Soft coke	Hard coke	Non-volatile	Total wt. reduction
HZSM-5 (pure)	1.4	0.1	0.1	0.1	1.7
HZSM-5 (spent)	0.6	2.8	2.2	0.5	6.1

the splitting of 1-propanol into smaller molecules and thus promotes coke deposition. Xia, Huang[49] confirmed these results in their study. Compared to the HZSM-5, the Ni/ZSM-5 showed an increased hard coke content, which reached up to 3.01 wt%, together with 2.49 wt% of soft coke. The catalytic role of nickel in the oxidation of coke leads to improved burning of soft coke on the Ni/ZSM-5 catalyst attributed to its redox properties and the large surface area of the Ni/HZSM-5.[50] As a result, there is less accumulation of soft coke on the catalyst surface, which improves long-chain HCs selectivity. This is reflected in the broader product distribution observed with the Ni/ZSM-5. The formation of soft coke in this scenario results from the accumulation of intermediates on the catalyst surface. These intermediates lead to the formation of long-chain HCs and coke during further polymerisation, which might ultimately lead to the Ni/HZSM-5 deactivation.[51–53]

The pure HZSM-5 catalyst, which had not been used previously, showed the least weight loss as it was not exposed reaction process, hence no coke formation. As can be seen in Fig. 7, the DTA curve shows a higher peak for the Ni/HZSM-5, indicating a susceptibility to coke formation. This result agrees with the higher coke formation observed in the TGA analysis for Ni/HZSM-5. From the coke study, it can be deduced that the conversion of 1-propanol to HC for the Ni/HZSM-5 catalyst could decrease with longer time-on-stream (TOS) due to the formation of hard coke. The addition of Ni species leads to a decrease in strong acidity and an increase in pore size, both of which contribute to the improved selectivity of this catalyst for long-chain HCs. The reduced BAS results in less cracking and less condensation, which favours the formation of long-chain HCs, which tend to block the catalyst pores.[54] Consequently, high coke deposition on the Ni/HZSM-5 increases the diffusion resistance and minimises the available active sites, which in turn contributes to increased catalyst deactivation. A summary of the coke deposition and weight loss of the spent catalysts can be found in Table 2.

3.2.3. Coke composition study. FTIR spectroscopy was used to identify the binding vibrations of the spent (coked) catalyst and adsorbed hydrocarbons on the spent catalysts after 1-propanol conversion. The identification of coke can be deduced from the characteristic spectral bands of the hydrocarbon molecules. The important regions in the FTIR spectrum that are of interest for the characterisation of coke are the 1300–1700 cm^{-1} and 2800–3100 cm^{-1} regions (Fig. 8). The vibrations in 1300–1700 cm^{-1} are due to the presence of polycondensed aromatics, conjugated olefins and some aliphatic bending modes, while the vibrations in the 2800–3100 cm^{-1} region indicate aliphatics (asymmetric and symmetric stretching) and single ring aromatics (Table 3).[55–58] However, these values are approximate and may contain slight deviations due to certain variables. The dominant band at 1625 cm^{-1} was more pronounced in the Ni/HZSM-5, indicating the formation of more double-bonded or olefinic HCs in contrast to Ni/HZSM-5. In addition, the Ni-doped catalyst exhibited a higher abundance of CH_3 groups and CH_2 groups than the unmodified HZSM-5. These results are consistent with previous studies,[55,56,58] indicating that metal species promote the formation of olefinic hydrocarbons and long aliphatic chains in the coke composition through processes such as aromatisation and oligomerisation. The observed trends in reaction products in Fig. 1a and b and adsorbed hydrocarbons are consistent with expectations for the 1-propanol conversion.[58–60] The data presented show a correlation between olefin production and conversion level, suggesting that olefins act as reaction intermediates while heavy aliphatic and aromatic compounds are end products, which is consistent with the general mechanism of 1-propanol conversion.

In contrast to unmodified HZSM-5, the deactivation of Ni/HZSM-5 can be attributed to the poisoning of the active sites by coke deposits. Hydrocarbon molecules can be dehydrated, fragmented, and polymerised during the reaction, forming coke that is attached to the surface of the catalyst and hinders the active sites. With nickel-doped HZSM-5, coke formation is more evident due to the high performance of Ni in promoting dehydrogenation, which produces carbonaceous species. Coking tends to occur at more acidic sites and accelerates the catalyst deactivation. This deactivation is due to coke deposition, which

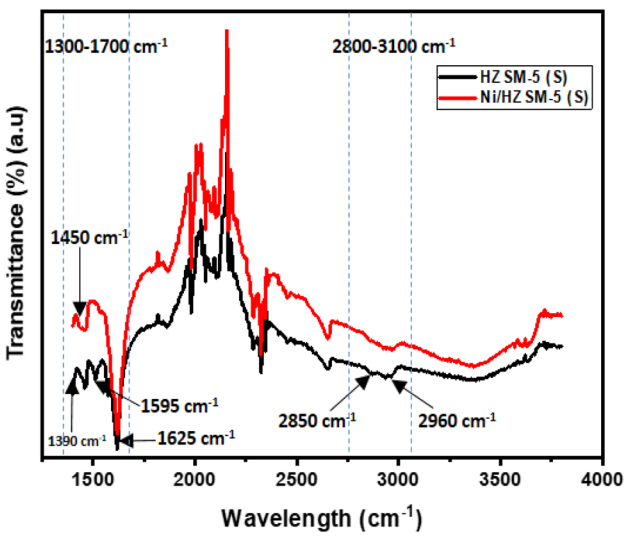

Fig. 8 Composition of coke deposited on spent catalysts (FTIR spectra: 1250–3750 cm^{-1} region).

Table 3 FTIR wavenumbers and functional group representations for unused and spent catalysts

FTIR wavenumber (cm^{-1})	Representation/functional groups	Ref.
1300–1700 range	Polycondensed aromatics (PCA), conjugated olefins, and aliphatic	55–58
2800–3100 range	Aliphatics and single-ring aromatics	
1390	Terminal $-CH_3$ groups	
1450	Aliphatics and alkyl aromatics	
1595	Coke band or PCA	
1620	Double bonds or olefins	
2850	$-CH_2$ groups	
2960	$-CH_3$ groups	

reduces the surface area of the catalyst and hinders reactants' accessibility to the active sites, hence reducing catalytic performance.[61,62]

The findings of this study align with those reported by Wan, Li,[63] where two ZSM-5 catalysts, one with nanocrystals around 100 nm in size and the other with microcrystals approximately 13 μm, were synthesised and evaluated for methanol-to-gasoline (MTG) conversion efficiency, with particular emphasis on coke formation and characteristics. When methanol conversion dropped to 50%, marking the catalyst's effective lifespan, the nanocrystal catalyst accumulated 31.1 wt% coke, compared to 14.1 wt% in the microcrystal catalyst. Remarkably, the nanocrystal catalyst's lifespan was nearly seven times longer than that of the microcrystal counterpart. This difference in longevity was investigated by analysing the rate of internal coke formation and the external coke structure using nitrogen physisorption, TGA, and TEM techniques. Findings showed that internal coke in the microcrystal catalyst accumulated more rapidly, leading to faster active site coverage and pore blockage, which in turn hastened deactivation. Conversely, coke mainly formed on the nanocrystal catalyst's exterior, producing a porous, graphitic layer that minimally impacted catalytic performance. After regeneration, the coke-laden nanocrystal catalyst demonstrated an extended lifespan in repeated tests under similar conditions, likely due to decreased aluminium content enhancing catalytic durability.[63]

To mitigate coke deposition and prevent deactivation in metal-doped ZSM-5 zeolite catalysts during the conversion of alcohol to fuel-range hydrocarbons, several strategies can be adopted to enhance coke resistance. By improving mesoporosity, the hierarchical pore system will enhance the diffusion of larger hydrocarbon intermediates, effectively reducing internal coke formation, which often clogs micropores in conventional ZSM-5. In addition, alumina coating has been shown to restrict coke formation on the surface, further improving resistance to carbon deposition without compromising active internal sites.[64,65] Carefully optimising reaction conditions can minimise coke deposition, particularly by reducing the formation of hard coke, and enable longer operating cycles between regenerations.[66,67] Furthermore, a corrective coke mitigation approach can be applied. This involves catalyst regeneration through a dual-stage coke combustion approach, in which soft coke is removed by sweeping with N_2 or combustion under mild conditions to maintain structural stability while hard coke is selectively oxidised at controlled temperatures not exceeding the calcination threshold. This method preserves the catalyst framework and extends its lifespan and performance without the harsh thermal treatments (>700 °C) that often lead to the dealumination of ZSM-5 catalysts.[68] Through these advanced strategies, the metal-doped ZSM-5 catalyst can achieve improved performance and durability in alcohol conversion, maintaining high activity and selectivity for fuel-range hydrocarbons with minimised coke-related deactivation.

The findings on coke deposition in ZSM-5 catalysts during 1-propanol conversion to fuel have promising implications for industrial applications and commercial catalyst development. The hierarchical structure of ZSM-5, which demonstrated resistance to coke formation, suggests a scalable approach to creating catalysts that retain activity over extended use. This could reduce regeneration cycles, lowering operational costs and enhancing efficiency for continuous fuel production. The study's insights on reaction conditions and metal-incorporated catalyst design offer a roadmap for developing commercial catalysts that minimise coke formation while maintaining high conversion rates. By optimizing catalyst structure and operational conditions, these findings provide a foundation for producing durable catalysts suitable for industrial alcohol-to-fuel processes, such as alcohol-to-gasoline or alcohol-to-jet fuel, supporting sustainable fuel production on a larger scale.

4. Conclusion

The effect of nickel modification on the coke formation of hierarchical HZSM-5 catalysts for the conversion of 1-propanol into fuel blendstocks was investigated at 350–400 °C and 7–12 h^{-1}. The evaluation of these catalysts in the conversion of 1-propanol showed a consistent conversion of >98% for both catalysts. While both catalysts showed significant selectivity for jet fuel and gasoline blends at >80 and >50%, respectively, Ni/HZSM-5 improved BTX production (19.4%). The stability study indicates that HZSM-5 offers greater stability and lower deactivation over time, whereas Ni/HZSM-5 shows higher initial activity, especially for jet fuel, but with a tendency for faster deactivation. These findings suggest that hierarchical HZSM-5 may be preferable for continuous long-term operations, while Ni/HZSM-5 could be beneficial for shorter-term processes where high jet fuel output is desired. The coke study showed that

HZSM-5 exhibited coke deposition of 2.80% and 2.24% at 200–400 °C and 400–600 °C, respectively. Ni/HZSM-5 showed higher deposition of hard coke (3.01 wt%) than soft coke (2.49 wt%), which can be attributed to the catalytic role of Ni in the oxidation of soft coke, resulting in improved selectivity for long-chain HCs. These results were confirmed by a DTA analysis, which showed that the Ni-doped catalyst has a higher affinity for coking and is more susceptible to deactivation than the unmodified catalyst. These results show the effect of Ni doping on coke deposition and catalyst performance. The coke composition showed that spent catalysts comprise polycondensed aromatics, conjugated olefins and some aliphatics. This study provides valuable insights for biomass and biomass-derived technology developers as it contributes to the understanding of coke formation, catalyst deactivation and lifetime. This understanding will facilitate the development of more effective and stable hierarchical catalysts, leading to lower process costs in the long term.

The ESI† file provides detailed characterization results of the fresh catalysts.

Data availability

Data for this study is available from the authors on request.

Author contributions

Conceptualization: [Ifeanyi Michael Smarte Anekwe], methodology: [Ifeanyi Michael Smarte Anekwe], formal analysis and investigation: [Ifeanyi Michael Smarte Anekwe], validation: [Ifeanyi Michael Smarte Anekwe], Writing – original draft preparation: [Ifeanyi Michael Smarte Anekwe], Writing – review and editing: [Yusuf Makarfi Isa], resources: [Yusufi Makarfi Isa], supervision: [Yusufi Makarfi Isa].

Conflicts of interest

The authors have no competing interests to declare that are relevant to the content of this article.

References

1 I. M. S. Anekwe, E. K. Tetteh, S. Akpasi, S. J. Atuman, E. K. Armah and Y. M. Isa, Carbon dioxide capture and sequestration technologies–current perspective, challenges and prospects, *Green Sustainable Process Chem. Environ. Eng. Sci.*, 2023, 481–516.

2 G. W. Huber, S. Iborra and A. Corma, Synthesis of transportation fuels from biomass: chemistry, catalysts, and engineering, *Chem. Rev.*, 2006, **106**(9), 4044–4098.

3 M. H. Langholtz, B. J. Stokes, L. M. Eaton. *2016 Billion-Ton Report: Advancing Domestic Resources for a Thriving Bioeconomy*. EERE Publication and Product Library, Washington, DC (United States); 2016.

4 A. Corma, S. Iborra and A. Velty, Chemical routes for the transformation of biomass into chemicals, *Chem. Rev.*, 2007, **107**(6), 2411–2502.

5 Y.-C. Lin and G. W. Huber, The critical role of heterogeneous catalysis in lignocellulosic biomass conversion, *Energy Environ. Sci.*, 2009, **2**(1), 68–80.

6 P. Gallezot, Conversion of biomass to selected chemical products, *Chem. Soc. Rev.*, 2012, **41**(4), 1538–1558.

7 Y. Zhi, H. Shi, L. Mu, Y. Liu, D. Mei, D. M. Camaioni, *et al.*, Dehydration Pathways of 1-Propanol on HZSM-5 in the Presence and Absence of Water, *J. Am. Chem. Soc.*, 2015, **137**(50), 15781–15794.

8 A. W. Lepore, Z. Li, B. H. Davison, G. S. Foo, Z. Wu and C. K. Narula, Catalytic Dehydration of Biomass Derived 1-Propanol to Propene over M-ZSM-5 (M = H, V, Cu, or Zn), *Ind. Eng. Chem. Res.*, 2017, **56**(15), 4302–4308.

9 I. M. S. Anekwe, B. Oboirien and Y. M. Isa, Performance evaluation of a newly developed transition metal-doped HZSM-5 zeolite catalyst for single-step conversion of C 1–C 3 alcohols to fuel-range hydrocarbons, *Energy Adv.*, 2024, **3**(6), 1314–1328.

10 C. P. Nash, A. Ramanathan, D. A. Ruddy, M. Behl, E. Gjersing, M. Griffin, *et al.*, Mixed alcohol dehydration over Brønsted and Lewis acidic catalysts, *Appl. Catal., A*, 2016, **510**, 110–124.

11 K. K. Ramasamy and Y. Wang, Catalyst activity comparison of alcohols over zeolites, *J. Energy Chem.*, 2013, **22**(1), 65–71.

12 U. V. Mentzel, S. Shunmugavel, S. L. Hruby, C. H. Christensen and M. S. Holm, High Yield of Liquid Range Olefins Obtained by Converting i-Propanol over Zeolite H-ZSM-5, *J. Am. Chem. Soc.*, 2009, **131**(46), 17009–17013.

13 Z. Li, E. Jiang, X. Xu, Y. Sun and R. Tu, Hydrodeoxygenation of phenols, acids, and ketones as model bio-oil for hydrocarbon fuel over Ni-based catalysts modified by Al, La and Ga, *Renewable Energy*, 2020, **146**, 1991–2007.

14 A. Kumar, Ethanol Decomposition and Dehydrogenation for Hydrogen Production: A Review of Heterogeneous Catalysts, *Ind. Eng. Chem. Res.*, 2021, **60**(46), 16561–16576.

15 I. M. S. Anekwe, B. Oboirien and Y. M. Isa, Catalytic conversion of bioethanol over cobalt and nickel-doped HZSM-5 zeolite catalysts, *Biofuels, Bioprod. Biorefin.*, 2024, **18**(3), 686–700.

16 S. Lycourghiotis, E. Kordouli, K. Bourikas, C. Kordulis and A. Lycourghiotis, The role of promoters in metallic nickel catalysts used for green diesel production: a critical review, *Fuel Process. Technol.*, 2023, **244**, 107690.

17 I. M. S. Anekwe, Y. M. Isa and B. Oboirien, Bioethanol as a Potential Eco-friendlier Feedstock for Catalytic Production of Fuels and Petrochemicals, *J. Chem. Technol. Biotechnol.*, 2023, **98**(9), 2077–2094.

18 D. Mores, E. Stavitski, M. H. F. Kox, J. Kornatowski, U. Olsbye and B. M. Weckhuysen, Space- and Time-Resolved In-situ Spectroscopy on the Coke Formation in Molecular Sieves: Methanol-to-Olefin Conversion over H-ZSM-5 and H-SAPO-34, *Chem.–Eur. J.*, 2008, **14**(36), 11320–11327.

19 M. Guisnet and P. Magnoux, Coking and deactivation of zeolites: influence of the pore structure, *Appl. Catal.*, 1989, **54**(1), 1–27.

20 U. Olsbye, S. Svelle, M. Bjørgen, P. Beato, T. V. W. Janssens, F. Joensen, *et al.*, Conversion of Methanol to Hydrocarbons: How Zeolite Cavity and Pore Size Controls Product Selectivity, *Angew. Chem., Int. Ed.*, 2012, **51**(24), 5810–5831.
21 F. Bleken, W. Skistad, K. Barbera, M. Kustova, S. Bordiga, P. Beato, *et al.*, Conversion of methanol over 10-ring zeolites with differing volumes at channel intersections: comparison of TNU-9, IM-5, ZSM-11 and ZSM-5, *Phys. Chem. Chem. Phys.*, 2011, **13**(7), 2539–2549.
22 S. Müller, Y. Liu, M. Vishnuvarthan, X. Sun, A. C. van Veen, G. L. Haller, *et al.*, Coke formation and deactivation pathways on H-ZSM-5 in the conversion of methanol to olefins, *J. Catal.*, 2015, **325**, 48–59.
23 P. Dejaifve, A. Auroux, P. C. Gravelle, J. C. Védrine, Z. Gabelica and E. G. Derouane, Methanol conversion on acidic ZSM-5, offretite, and mordenite zeolites: A comparative study of the formation and stability of coke deposits, *J. Catal.*, 1981, **70**(1), 123–136.
24 B. P. C. Hereijgers, F. Bleken, M. H. Nilsen, S. Svelle, K.-P. Lillerud, M. Bjørgen, *et al.*, Product shape selectivity dominates the Methanol-to-Olefins (MTO) reaction over H-SAPO-34 catalysts, *J. Catal.*, 2009, **264**(1), 77–87.
25 Q. Qian, J. Ruiz-Martínez, M. Mokhtar, A. M. Asiri, S. A. Al-Thabaiti, S. N. Basahel, *et al.*, Single-Particle Spectroscopy of Alcohol-to-Olefins over SAPO-34 at Different Reaction Stages: Crystal Accessibility and Hydrocarbons Reactivity, *ChemCatChem*, 2014, **6**(3), 772–783.
26 A. T. Aguayo, A. E. Sd Campo, A. G. Gayubo, A. Tarrío and J. Bilbao, Deactivation by coke of a catalyst based on a SAPO-34 in the transformation of methanol into olefins, *J. Chem. Technol. Biotechnol.*, 1999, **74**(4), 315–321.
27 M. Bjørgen, S. Svelle, F. Joensen, J. Nerlov, S. Kolboe, F. Bonino, *et al.*, Conversion of methanol to hydrocarbons over zeolite H-ZSM-5: On the origin of the olefinic species, *J. Catal.*, 2007, **249**(2), 195–207.
28 H. Schulz, "Coking" of zeolites during methanol conversion: Basic reactions of the MTO-, MTP- and MTG processes, *Catal. Today*, 2010, **154**(3), 183–194.
29 F. L. Bleken, K. Barbera, F. Bonino, U. Olsbye, K. P. Lillerud, S. Bordiga, *et al.*, Catalyst deactivation by coke formation in microporous and desilicated zeolite H-ZSM-5 during the conversion of methanol to hydrocarbons, *J. Catal.*, 2013, **307**, 62–73.
30 Y. Sun, T. Ma, L. Zhang, Y. Song, Y. Shang, Y. Zhai, *et al.*, The influence of zoned Al distribution of ZSM-5 zeolite on the reactivity of hexane cracking, *Mol. Catal.*, 2020, **484**, 110770.
31 M. Guisnet and P. Magnoux, Fundamental description of deactivation and regeneration of acid zeolites, *Stud. Surf. Sci. Catal.*, 1994, **88**, 53–68.
32 A. G. Gayubo, A. M. Tarrío, A. T. Aguayo, M. Olazar and J. Bilbao, Kinetic modelling of the transformation of aqueous ethanol into hydrocarbons on a HZSM-5 zeolite, *Ind. Eng. Chem. Res.*, 2001, **40**(16), 3467–3474.
33 A. T. Aguayo, A. G. Gayubo, A. Atutxa, M. Olazar and J. Bilbao, Catalyst deactivation by coke in the transformation of aqueous ethanol into hydrocarbons. Kinetic modeling and acidity deterioration of the catalyst, *Ind. Eng. Chem. Res.*, 2002, **41**(17), 4216–4224.
34 A. G. Gayubo, A. Alonso, B. Valle, A. T. Aguayo, M. Olazar and J. Bilbao, Hydrothermal stability of HZSM-5 catalysts modified with Ni for the transformation of bioethanol into hydrocarbons, *Fuel*, 2010, **89**(11), 3365–3372.
35 A. G. Gayubo, A. Alonso, B. Valle, A. T. Aguayo, M. Olazar and J. Bilbao, Kinetic modelling for the transformation of bioethanol into olefins on a hydrothermally stable Ni–HZSM-5 catalyst considering the deactivation by coke, *Chem. Eng. J.*, 2011, **167**(1), 262–277.
36 J. Sun and Y. Wang, Recent advances in catalytic conversion of ethanol to chemicals, *ACS Catal.*, 2014, **4**(4), 1078–1090.
37 C. D. Chang, MTG revisited, *Studies in Surface Science and Catalysis*, Elsevier; 1991, vol. 61, p. 393–404.
38 C. Wang, X. Zhang, Q. Liu, Q. Zhang, L. Chen and L. Ma, A review of conversion of lignocellulose biomass to liquid transport fuels by integrated refining strategies, *Fuel Process. Technol.*, 2020, **208**, 106485.
39 W. Deng, Y. Feng, J. Fu, H. Guo, Y. Guo, B. Han, *et al.*, Catalytic conversion of lignocellulosic biomass into chemicals and fuels, *Green Energy Environ.*, 2023, **8**(1), 10–114.
40 L. P. S. Vandenberghe, K. K. Valladares-Diestra, G. A. Bittencourt, L. A. Zevallos Torres, S. Vieira, S. G. Karp, *et al.*, Beyond sugar and ethanol: The future of sugarcane biorefineries in Brazil, *Renewable Sustainable Energy Rev.*, 2022, **167**, 112721.
41 A. Jawad and S. Ahmed, Analysis and process evaluation of metal dopant (Zr, Cr)-promoted Ga-modified ZSM-5 for the oxidative dehydrogenation of propane in the presence and absence of CO 2, *RSC Adv.*, 2023, **13**(16), 11081–11095.
42 S. Kim, E. Sasmaz, R. Pogaku and J. Lauterbach, Effects of reaction conditions and organic sulfur compounds on coke formation and HZSM-5 catalyst performance during jet propellant fuel (JP-8) cracking, *Fuel*, 2020, **259**, 116240.
43 K.-Y. Lee, M.-Y. Kang and S.-K. Ihm, Deactivation by coke deposition on the HZSM-5 catalysts in the methanol-to-hydrocarbon conversion, *J. Phys. Chem. Solids*, 2012, **73**(12), 1542–1545.
44 T. Meng, D. Mao, Q. Guo and G. Lu, The effect of crystal sizes of HZSM-5 zeolites in ethanol conversion to propylene, *Catal. Commun.*, 2012, **21**, 52–57.
45 P. Ciambelli, V. Palma and A. Ruggiero, Low temperature catalytic steam reforming of ethanol. 1. The effect of the support on the activity and stability of Pt catalysts, *Appl. Catal., B*, 2010, **96**(1–2), 18–27.
46 M. Díaz, E. Epelde, J. Valecillos, S. Izaddoust, A. T. Aguayo and J. Bilbao, Coke deactivation and regeneration of HZSM-5 zeolite catalysts in the oligomerization of 1-butene, *Appl. Catal., B*, 2021, **291**, 120076.
47 I. M. S. Anekwe, M. Chetty, L. Khotseng, S. L. Kiambi, L. Maharaj, B. Oboirien, *et al.*, Stability, deactivation and regeneration study of a newly developed HZSM-5 and Ni-doped HZSM-5 zeolite catalysts for ethanol-to-hydrocarbon conversion, *Catal. Commun.*, 2024, **186**, 106802.

48 M. He, M.-F. Ali, Y.-Q. Song, X.-L. Zhou, J. A. Wang, X.-Y. Nie, *et al.*, Study on the deactivation mechanism of HZSM-5 in the process of catalytic cracking of n-hexane, *Chem. Eng. J.*, 2023, **451**, 138793.

49 W. Xia, Y. Huang, C. Ma, S. Li, X. Wang, K. Chen, *et al.*, Multiple important roles of phosphorus modification on the ZSM-5 in ethanol to olefin reaction: Acidity adjustment, hydrothermal stability and anti-coking, *Fuel*, 2023, **341**, 127675.

50 S. Kawi, Y. Kathiraser, J. Ni, U. Oemar, Z. Li and E. T. Saw, Progress in synthesis of highly active and stable nickel-based catalysts for carbon dioxide reforming of methane, *ChemSusChem*, 2015, **8**(21), 3556–3575.

51 Y. Li, C. Zhang, Y. Liu, S. Tang, G. Chen, R. Zhang, *et al.*, Coke formation on the surface of Ni/HZSM-5 and Ni-Cu/HZSM-5 catalysts during bio-oil hydrodeoxygenation, *Fuel*, 2017, **189**, 23–31.

52 H. O. Mohamed, R. K. Parsapur, I. Hita, J. L. Cerrillo, A. Ramírez, K.-W. Huang, *et al.*, Stable and reusable hierarchical ZSM-5 zeolite with superior performance for olefin oligomerization when partially coked, *Appl. Catal., B*, 2022, **316**, 121582.

53 H. K. G. Singh, S. Yusup, A. T. Quitain, B. Abdullah, M. Ameen, M. Sasaki, *et al.*, Biogasoline production from linoleic acid *via* catalytic cracking over nickel and copper-doped ZSM-5 catalysts, *Environ. Res.*, 2020, **186**, 109616.

54 H. Zhang, S. Shao, R. Xiao, D. Shen and J. Zeng, Characterization of coke deposition in the catalytic fast pyrolysis of biomass derivates, *Energy Fuels*, 2014, **28**(1), 52–57.

55 H. G. Karge, W. Nießen and H. Bludau, In-situ FTIR measurements of diffusion in coking zeolite catalysts, *Appl. Catal., A*, 1996, **146**(2), 339–349.

56 L. Palumbo, F. Bonino, P. Beato, M. Bjørgen, A. Zecchina and S. Bordiga, Conversion of Methanol to Hydrocarbons: Spectroscopic Characterization of Carbonaceous Species Formed over H-ZSM-5, *J. Phys. Chem. C*, 2008, **112**(26), 9710–9716.

57 J. Robertson, Diamond-like amorphous carbon, *Mater. Sci. Eng., R*, 2002, **37**(4), 129–281.

58 J. Valecillos, H. Vicente, A. G. Gayubo, A. T. Aguayo and P. Castaño, Spectro-kinetics of the methanol to hydrocarbons reaction combining online product analysis with UV–vis and FTIR spectroscopies throughout the space time evolution, *J. Catal.*, 2022, **408**, 115–127.

59 J. Valecillos, E. Epelde, J. Albo, A. T. Aguayo, J. Bilbao and P. Castaño, Slowing down the deactivation of H-ZSM-5 zeolite catalyst in the methanol-to-olefin (MTO) reaction by P or Zn modifications, *Catal. Today*, 2020, **348**, 243–256.

60 S. Ilias and A. Bhan, Mechanism of the catalytic conversion of methanol to hydrocarbons, *ACS Catal.*, 2013, **3**(1), 18–31.

61 S. Pinjari, M. K. Kumaravelan, V. C. Peddy, S. Gandham, J. Patruni, S. Velluru, *et al.*, Maximizing the production of hydrogen and carbon nanotubes: Effect of Ni and reaction temperature, *Int. J. Hydrogen Energy*, 2018, **43**(5), 2781–2793.

62 A. Maia, B. Oliveira, P. Esteves, B. Louis, Y. Lam and M. Pereira, Isobutane and n-butane cracking on Ni-ZSM-5 catalyst: Effect on light olefin formation, *Appl. Catal., A*, 2011, **403**(1–2), 58–64.

63 Z. Wan, G. K. Li, C. Wang, H. Yang and D. Zhang, Relating coke formation and characteristics to deactivation of ZSM-5 zeolite in methanol to gasoline conversion, *Appl. Catal., A*, 2018, **549**, 141–151.

64 A. Sarris S, H. Symoens S, N. Olahova, M.-F. Reyniers, B. Marin G and M. Van Geem K, Alumina-based coating for coke reduction in steam crackers, *Materials*, 2020, **13**(9), 2025.

65 Y. Jang, S. M. Lee, B. Jeong and S. S. Kim, Enhanced Al2O3 Interlayer Coating for Inhibition of Filamentous Coke Formation in n-Dodecane Cracking Reaction, *Ind. Eng. Chem. Res.*, 2023, **62**(46), 19437–19447.

66 W. Di, A. Achour, P. H. Ho, S. Ghosh, O. Pajalic, L. Josefsson, *et al.*, Modulating the Formation of Coke to Improve the Production of Light Olefins from CO2 Hydrogenation over In2O3 and SSZ-13 Catalysts, *Energy Fuels*, 2023, **37**(22), 17382–17398.

67 M. F. Reyniers, Y. Tang and G. B. Marin, Influence of coke formation on the conversion of hydrocarbons: II. i-Butene on HY-zeolites, *Appl. Catal., A*, 2000, **202**(1), 65–80.

68 J. Zhou, J. Zhao, J. Zhang, T. Zhang, M. Ye and Z. Liu, Regeneration of catalysts deactivated by coke deposition: A review, *Chin. J. Catal.*, 2020, **41**(7), 1048–1061.